

# Ultrawideband Vector Antennas for Sensing and Positioning

Sandeep H. Krishnamurthy, Anand Konanur, Gianluca Lazzi, and Brian L. Hughes

Email: {shkrishn,askonanu,lazzi,blhughes}@ncsu.edu

**Abstract**—Over the last decade, there has been a growing recognition that ultra-wideband (UWB) radios offer several unique capabilities that can enable new sensing, positioning, and communication applications. Most UWB systems currently use single- or dual-polarized antennas, which can measure at most two components of the received electromagnetic (EM) signal. Since the received signal consists of six field components, however, potentially useful information is neglected. In principle, a “vector antenna” that can independently detect or excite three or more EM field components enables the UWB system to access additional signaling dimensions, which can be used to enhance performance in the same way as antenna arrays. In this paper, we consider the potential advantages of UWB vector antenna systems for range and direction-of-arrival (DOA) estimation. We first introduce a general model for an UWB vector antenna system that incorporates the possibility of arbitrary space- and frequency-selective antenna coupling. We then use this model to derive a frequency-domain Cramér-Rao lower bound on the position error covariance for arbitrary polarized UWB signals. For two particular 3-element UWB vector antennas, we then use the bound as a design criterion to derive optimal UWB polarized signals that minimize a lower bound on mean-square angular estimation error.

**Keywords:** Ultra-wideband Signaling, Ranging, Direction-of-arrival estimation, Cramér-Rao Bound

## I. INTRODUCTION

Over the last decade, there has been a growing recognition that ultra-wideband (UWB) radios offer several unique capabilities that can enable a host of new sensing, positioning, and communication applications. UWB has long been used in ground-penetrating radars, and is now being applied to new imaging devices (e.g. Time Domain’s RadarVision) which enable law enforcement, fire and rescue personnel to see through walls and debris during emergencies. These devices can also improve safety in construction by locating steel bars, electrical wiring, and utility pipes hidden inside walls or underground. Recently, UWB medical imaging systems have been proposed which achieve unprecedented resolution in mammograms. The precise ranging capability of UWB can provide accurate tracking for many applications, such as remote inventory, personnel and asset tracking, and collision avoidance radars and air bag proximity detectors for automobiles. In communications, UWB can transmit very high

data rates over short distances without suffering the effects of multipath, and can relieve congested spectrum by effectively opening up new frequency bands in the noise floor (consistent with Part 15 rules, [1]). Several standardization efforts are now underway (e.g., IEEE 802.15.3 and 802.15.3 Sg3a) to develop UWB wireless personal area networks and local area networks that can overlay and co-exist with existing wireless systems.

Most work on ultra-wideband systems has thus far focused on single-polarized electric dipole antennas. Dual-polarized antennas have been studied in certain radar applications, such as ground-penetrating and synthetic-aperture radars (e.g., [5], [3], [6] and references therein). Single- and dual-polarized antennas can measure at most two components of the received signal. Since the signal detected at the receiver consists of six electromagnetic field components, however, these antennas neglect data that might be available to improve the performance of the sensing, positioning, and communications algorithms. A “vector antenna” that can independently detect or excite three or more EM field components enables the UWB system to access additional signaling dimensions, which can be used to enhance performance in the same way as antenna arrays.

In principle, a 6-element vector antenna might be constructed by combining three electric dipoles to detect the electric field components, with three magnetic dipoles (i.e., loops) to detect the magnetic field components. Vector antennas that respond to all six EM field components have been investigated [11], [14], however, these devices are relatively *narrowband* ( $< 30$  MHz) and extremely large (many times the wavelength). The use of such antennas to estimate the direction-of-arrival of electromagnetic signals in line-of-sight propagation has been extensively investigated in narrowband systems [7], [9], [8]. There is a rich literature on beamforming with spatial arrays of scalar UWB antennas (e.g., [10], [12], [15]).

In this paper, we develop some tools for the design of UWB systems for precise location estimation. A generalized asymptotic expression for the Cramér-Rao bound is derived in section II. Section III presents a signal model for a vector antenna receiver. The exact error bounds are given in IV and the optimal signal design criterion is discussed in V. The notation used is as follows. If  $A$  is complex matrix,  $A^\dagger$  is the conjugate-transpose of  $A$ .  $E[\cdot]$  is the expectation operator,  $\text{Tr}[\cdot]$  is the trace operator,  $\mathcal{CN}(\mathbf{m}, C)$  is a circularly symmetric complex Gaussian random variable with mean  $\mathbf{m}$  and covariance  $C$ .

<sup>1</sup>The authors are with Center for Advanced Computing and Communication, Dept. of Electrical and Computer Engineering, North Carolina State University, Raleigh NC 27606.

<sup>2</sup>This work was supported in part by the National Science Foundation under grants CCR-013017 and CCR-0381706, and by the Center for Advanced Computing and Communication.

## II. FREQUENCY-DOMAIN CRAMÉR-RAO BOUND

Consider the discrete-time complex observation

$$\mathbf{y}(t) = \mathbf{m}(t, \vartheta) + \mathbf{n}(t, \vartheta), \quad t = 1, \dots, N$$

where  $\mathbf{m}(t, \vartheta)$  is the  $r \times 1$  deterministic signal vector, which depends on the unknown  $p$ -dimensional parameter vector  $\vartheta$ , and  $\mathbf{n}(t, \vartheta)$  is a proper<sup>1</sup> zero-mean complex Gaussian process with covariance dependent on  $\vartheta$ . To evaluate the Fisher Information Matrix (FIM), it is convenient to stack the observations into a single  $Nr \times 1$  observation  $\mathbf{y} = (\mathbf{y}(1)^T, \dots, \mathbf{y}(N)^T)^T$  in which case the FIM is given by [4, pg. 525]

$$[\mathcal{I}(\vartheta)]_{k,l} = 2\text{Re} \left[ \frac{\partial \mathbf{m}^H(\vartheta)}{\partial \vartheta_k} R^{-1}(\vartheta) \frac{\partial \mathbf{m}(\vartheta)}{\partial \vartheta_l} \right] + \text{Tr} \left\{ R^{-1}(\vartheta) \frac{\partial R(\vartheta)}{\partial \vartheta_k} R^{-1}(\vartheta) \frac{\partial R(\vartheta)}{\partial \vartheta_l} \right\}$$

where  $\mathbf{m}(\vartheta) = (\mathbf{m}(1, \vartheta)^T, \dots, \mathbf{m}(N, \vartheta)^T)^T$  and  $R(\vartheta)$  is the  $Nr \times Nr$  covariance of  $\mathbf{n}(\vartheta) = (\mathbf{n}(1, \vartheta)^T, \dots, \mathbf{n}(N, \vartheta)^T)^T$ .

Our main results are explicit formulas for the Cramér-Rao Bound (CRB), which provides a lower bound on the covariance matrix of any locally unbiased estimator of  $\vartheta$ . More specifically, if

$$C_{\hat{\vartheta}} = \mathcal{E} \left[ (\hat{\vartheta} - \vartheta)(\hat{\vartheta} - \vartheta)^T \right]$$

is the covariance of the estimation error, then the CRB

$$C_{\hat{\vartheta}} - \mathcal{I}^{-1}(\vartheta)$$

is non-negative definite.

If  $\mathbf{n}(t, \vartheta)$  is a stationary process for each  $\vartheta$ , then its covariance has a block Toeplitz structure

$$R(\vartheta) = \begin{bmatrix} T_0 & T_{-1} & \cdots & T_{-(N-1)} \\ T_1 & T_0 & \cdots & T_{-(N-2)} \\ \vdots & \vdots & \ddots & \vdots \\ T_{N-1} & T_{N-2} & \cdots & T_0 \end{bmatrix}$$

where  $T_k$  is the autocorrelation function

$$T_k = T_k(\vartheta) = \mathcal{E} \left[ \mathbf{n}(t+k, \vartheta) \mathbf{n}^H(t, \vartheta) \right].$$

Note that  $R(\vartheta)$  is Hermitian since  $T_k = T_{-k}^H$ .

We are interested in an asymptotic frequency-domain expression for the CRB in the limit as  $N$  becomes large. To this end, we introduce some notation: For any  $n \times n$  complex matrix  $A$ , the strong norm is defined as the spectral norm

$$\|A\| = \sup_{\mathbf{x}: \mathbf{x}^H \mathbf{x} = 1} (\mathbf{x}^H A \mathbf{x})^{1/2},$$

and the weak norm is defined to be the normalized Frobenius norm

$$|A| = (n^{-1} \text{Tr}[A^H A])^{1/2}.$$

<sup>1</sup>A stationary complex random process is proper if the pseudo-covariance  $\mathcal{E}[(\mathbf{n}(t+k) - \bar{\mathbf{n}}(t+k))(\mathbf{n}(t+k) - \bar{\mathbf{n}}(t+k))^T]$  vanishes for all  $k$  [13].

**Definition 1:** Two sequences of  $n \times n$  matrices,  $\{A_n\}$  and  $\{B_n\}$ , are said to be equivalent if there exists an  $M < \infty$  such that  $\|A_n\| \leq M$  and  $\|B_n\| \leq M$  and

$$\lim_{n \rightarrow \infty} |A_n - B_n| = 0.$$

Suppose that for all  $\vartheta$ , the discrete Fourier Transform

$$T(\omega, \vartheta) = \sum_{k=-\infty}^{\infty} T_k(\vartheta) e^{-jk\omega}$$

exists and is continuous in  $\omega \in (-\pi, \pi)$ . By Lemma A1 of the appendix,  $R(\vartheta)$  is asymptotically equivalent to the block circulant matrix

$$C_N(\vartheta) = (W_N \otimes I_r)^H D_N(T) (W_N \otimes I_r)$$

where  $W_n$  is the  $n \times n$  discrete Fourier Transform (DFT) matrix

$$[W_n]_{ij} = \frac{1}{\sqrt{n}} \exp\left(-\frac{2\pi(i-1)(j-1)}{n}\right),$$

$D_n(T)$  is the block diagonal matrix

$$D_N(T) = \begin{bmatrix} T(\omega_1, \vartheta) & O & \cdots & O \\ O & T(\omega_2, \vartheta) & \cdots & O \\ \vdots & \vdots & \ddots & \vdots \\ O & O & \cdots & T(\omega_N, \vartheta) \end{bmatrix}$$

and  $\omega_i = \exp\left(-\frac{2\pi(i-1)}{N}\right)$ .

Similarly, suppose that the discrete Fourier Transform of the sequence  $\left\{\frac{\partial T_k}{\partial \vartheta_l}\right\}$  exists and is equal to  $\frac{\partial T}{\partial \vartheta_l}(\omega, \vartheta)$  for all  $l$  and  $\vartheta$ , then

$$\frac{\partial R(\vartheta)}{\partial \vartheta_l} \sim (W_N \otimes I_r)^H D_N\left(\frac{\partial T}{\partial \vartheta_l}\right) (W_N \otimes I_r)$$

and if  $\sigma[T(\omega, \vartheta)] \geq c > 0$  for all  $\omega$  and  $\vartheta$ , then

$$R_N^{-1}(\vartheta) \sim (W_N \otimes I_r)^H D_N(T^{-1}) (W_N \otimes I_r)$$

Note that  $A_n \sim B_n$  and  $C_n \sim D_n$  implies  $A_n C_n \sim B_n D_n$  and

$$\lim_{n \rightarrow \infty} (1/n) \text{Tr}[A_n] = \lim_{n \rightarrow \infty} (1/n) \text{Tr}[B_n].$$

It follows that

$$\begin{aligned} & \lim_{N \rightarrow \infty} \frac{1}{N} \text{Tr} \left\{ R^{-1}(\vartheta) \frac{\partial R(\vartheta)}{\partial \vartheta_k} R^{-1}(\vartheta) \frac{\partial R(\vartheta)}{\partial \vartheta_l} \right\} \\ &= \lim_{N \rightarrow \infty} \frac{1}{N} \text{Tr} \left\{ C^{-1}(\vartheta) \frac{\partial C(\vartheta)}{\partial \vartheta_k} C^{-1}(\vartheta) \frac{\partial C(\vartheta)}{\partial \vartheta_l} \right\} \\ &= \lim_{N \rightarrow \infty} \frac{1}{N} \sum_{i=1}^N \text{Tr} \left\{ T^{-1}(\omega_i, \vartheta) \frac{\partial T(\omega_i, \vartheta)}{\partial \vartheta_k} T^{-1}(\omega_i, \vartheta) \frac{\partial T(\omega_i, \vartheta)}{\partial \vartheta_l} \right\} \\ &= \frac{1}{2\pi} \int_{-\pi}^{\pi} \text{Tr} \left\{ T^{-1}(\omega, \vartheta) \frac{\partial T(\omega, \vartheta)}{\partial \vartheta_k} T^{-1}(\omega, \vartheta) \frac{\partial T(\omega, \vartheta)}{\partial \vartheta_l} \right\} d\omega \end{aligned}$$

Similarly, defining the the  $r \times 1$  DFT of the signal as

$$M(\omega, \vartheta) = \sum_{t=-\infty}^{\infty} \mathbf{m}(t, \vartheta) e^{-jt\omega},$$

we can show that

$$\begin{aligned} & \lim_{N \rightarrow \infty} \frac{1}{N} \text{Re} \left[ \frac{\partial \mathbf{m}^H(\vartheta)}{\partial \vartheta_k} R^{-1}(\vartheta) \frac{\partial \mathbf{m}(\vartheta)}{\partial \vartheta_l} \right] \\ &= \frac{1}{2\pi} \int_{-\pi}^{\pi} \text{Re} \left\{ \frac{\partial M^H(\omega, \vartheta)}{\partial \vartheta_k} T^{-1}(\omega, \vartheta) \frac{\partial M(\omega, \vartheta)}{\partial \vartheta_l} \right\} d\omega. \end{aligned}$$

Then the asymptotic FIM is

$$\begin{aligned} & \lim_{N \rightarrow \infty} \frac{1}{N} [\mathcal{I}_N(\vartheta)]_{k,l} \\ &= \frac{1}{2\pi} \int_{-\pi}^{\pi} \left[ 2\text{Re} \left\{ \frac{\partial M^H(\omega, \vartheta)}{\partial \vartheta_k} T^{-1}(\omega, \vartheta) \frac{\partial M(\omega, \vartheta)}{\partial \vartheta_l} \right\} \right. \\ & \quad \left. + \text{Tr} \left\{ T^{-1}(\omega, \vartheta) \frac{\partial T(\omega, \vartheta)}{\partial \vartheta_k} T^{-1}(\omega, \vartheta) \frac{\partial T(\omega, \vartheta)}{\partial \vartheta_l} \right\} \right] d\omega \end{aligned}$$

### III. SIGNAL MODEL

We now introduce a simple model to describe the propagation of UWB polarized signals which captures many key features of the vector antenna environment, but which is tractable enough to allow an analysis of different antennas and beamforming algorithms. The model is based on the same assumptions as the narrowband sinusoidal model proposed by Nehorai and Paldi [7], but is here generalized to ultra-wideband, possibly non-sinusoidal signals.

Suppose first that the signal propagates by line-of-sight from the target to the UWB receiver. If the target is located at position  $(r, \theta, \varphi)$  in spherical coordinates centered at the receiver, as illustrated in Fig. 1, the signal arrives at the receiver from direction

$$\mathbf{u}_r = \begin{bmatrix} \cos \theta \sin \varphi \\ \sin \theta \sin \varphi \\ \cos \varphi \end{bmatrix} \quad (1)$$

where  $\theta$  and  $\varphi$  are the azimuth and elevation, respectively.

Let  $\mathbf{E}(t)$  and  $\mathbf{H}(t)$  denote the 3-dimensional electric and magnetic field vectors at the receiver, and suppose the target is sufficiently far from the receiver to justify a far-field approximation. Thus  $\mathbf{E}(t)$  and  $\mathbf{H}(t)$  constitute a plane ‘‘wave’’ which is constant on planes perpendicular to  $\mathbf{u}_r$ . For a finite-duration pulse propagating in a nonconductive, homogeneous, and isotropic medium,  $\mathbf{E}(t)$  and  $\mathbf{H}(t)$  must satisfy [7]

$$\eta \mathbf{H}(t) = -\mathbf{u}_r \times \mathbf{E}(t) \quad (2)$$

$$\mathbf{u}_r \cdot \mathbf{E}(t) = 0 \quad (3)$$

where  $\eta$  is the intrinsic impedance of the propagation medium.

The complete electromagnetic field at the receiver can be written as

$$\begin{bmatrix} \mathbf{E}(t) \\ \eta \mathbf{H}(t) \end{bmatrix} = B(\theta, \varphi) \mathbf{s}(t) \quad (4)$$

where  $\mathbf{s}(t) = [s_1(t), s_2(t)]^T$  is an arbitrary 2-dimensional

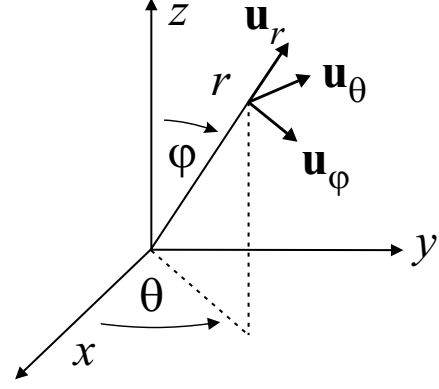


Fig. 1. The orthonormal triad  $(\mathbf{u}_r, \mathbf{u}_\varphi, \mathbf{u}_\theta)$

pulse and

$$B(\theta, \varphi) = \begin{bmatrix} -\sin \theta & \cos \theta \cos \varphi \\ \cos \theta & \sin \theta \cos \varphi \\ 0 & -\sin \varphi \\ \cos \theta \cos \varphi & \sin \theta \\ \sin \theta \cos \varphi & -\cos \theta \\ -\sin \varphi & 0 \end{bmatrix}. \quad (5)$$

From Fig. 1, it is clear that  $s_1(t)$  and  $s_2(t)$  are the horizontally and vertically polarized components of  $\mathbf{E}(t)$ , respectively. Recall that the electric field vector of a sinusoidal polarized signal describes an ellipse in the plane perpendicular to the direction of propagation (e.g., [17]). From (4), we see that the electric field of an ultra-wideband polarized signal also resides in the plane perpendicular to  $\mathbf{u}_r$ ; however, it can describe a more general motion.

In (5) we consider a vector antenna that detects all six components of the EM field. A vector antenna with  $m < 6$  outputs can be modeled by selecting the appropriate  $m$  rows from matrix  $B(\theta, \varphi)$  above. In this paper, we consider the problem of estimating the target position  $\vartheta = (\vartheta_1, \vartheta_2, \vartheta_3) = (r, \theta, \varphi)$  based on the data.

### IV. CRB FOR UWB VECTOR ANTENNAS

We now consider a special case relevant to the study of vector antennas. Recall that for a linear time invariant system the response can be written as a convolution, and that for a single reflector at a distance  $r$ , the received signal can be written as  $\mathbf{s}_r(t) = \mathbf{s}(t - 2r/c)$ . The response can be written as

$$\mathbf{m}(t, \vartheta) = B(t, \theta, \varphi) \star \mathbf{s}_r(t).$$

so that  $M(\omega, \vartheta) = B(\omega, \theta, \varphi) \mathbf{s}_r(\omega)$ . It seems reasonable to assume that frequency and angle dependencies are separable, so that  $B(\omega, \theta, \varphi) = G(\omega) B(\theta, \varphi)$ , where  $G(\omega)$  is a matrix that describes how the vector antenna responds to the incident EM field. If we assume that the noise is intrinsic to the sensors and independent of the target position, then  $T(\omega, \vartheta) =$

$T(\omega)$ . The asymptotic FIM can be written as

$$\frac{1}{\pi} \int_{-\pi}^{\pi} \text{Re} [\mathbf{D}^H(\omega, r, \theta, \varphi) G^H(\omega) T^{-1}(\omega) G(\omega) \mathbf{D}(\omega, r, \theta, \varphi)] d\omega$$

where  $\mathbf{D}(\omega, r, \theta, \varphi)$

$$= \begin{bmatrix} -(2/c)B(\theta, \varphi) \mathbf{s}'_r(\omega), B_\theta(\theta, \varphi) \mathbf{s}_r(\omega), B_\theta(\theta, \varphi) \mathbf{s}_r(\omega) \end{bmatrix}$$

where  $\mathbf{s}'_r(t)$  are the samples of  $s'(t - 2r/c)$ ,  $B_\theta(\theta, \varphi) = \partial B(\theta, \varphi) / \partial \theta$  and  $B_\varphi(\theta, \varphi) = \partial B(\theta, \varphi) / \partial \varphi$ .

If  $\hat{r}$ ,  $\hat{\theta}$  and  $\hat{\varphi}$  are unbiased estimates and  $\text{var}(\hat{r})$  is the Mean Squared Range Error (MSRE).  $\delta = \arccos(\mathbf{u} \cdot \hat{\mathbf{u}})$  is the angular error in the estimate, the mean squared angular error (MSAE) has a lower bound which can be expressed in terms of the CRB expressions for  $\theta$  and  $\varphi$   $E(\delta^2) = \text{var}(\delta) \geq \sin^2 \varphi \cdot \text{CRB}(\theta) + \text{CRB}(\varphi)$ .

#### A. Special Case: An UWB Tripole

Consider first the special case of a collection of three mutually orthogonal dipoles in the presence of spatially and temporally white noise. In this case, we have  $G^H(\omega) T^{-1}(\omega) G(\omega) = (1/\sigma^2) I_3$ . For the case of a UWB tripole, we have

$$B(\theta, \varphi) = \begin{bmatrix} -\sin \theta & \cos \theta \cos \varphi \\ \cos \theta & \sin \theta \cos \varphi \\ 0 & -\sin \varphi \end{bmatrix}$$

We define certain signal parameters for short-hand  $\mathcal{E} = \|\mathbf{s}_r\|^2$ ,  $s = \|\mathbf{s}_{r2}\|^2 / \|\mathbf{s}_r\|^2 = \mathcal{E}_2 / \mathcal{E}$ ,  $\omega^2 = \|\mathbf{s}'_r\|^2 / \|\mathbf{s}_r\|^2$ ,  $\rho = (2/\omega \mathcal{E}) \text{Re} \langle \mathbf{s}_{r2}, \mathbf{s}'_{r1} \rangle$ ,  $\mu = (1/\mathcal{E}) \text{Re} \langle \mathbf{s}_{r2}, \mathbf{s}_{r1} \rangle$ . Using the expression for asymptotic FIM, we have following bound for a locally unbiased estimator of the DOA:

$$\begin{aligned} \text{var}(\hat{r}) &\geq \frac{\sigma^2 c^2}{8\omega^2 \mathcal{E}} \frac{s(1 - s \sin^2 \varphi) - \mu^2 \sin^2 \varphi}{s(1 - s \sin^2 \varphi) - \mu^2 \sin^2 \varphi - s\rho^2 \cos^2 \varphi} \\ \text{var}(\hat{\theta}) &\geq \frac{\sigma^2}{2\mathcal{E}} \frac{s}{s(1 - s \sin^2 \varphi) - \mu^2 \sin^2 \varphi - s\rho^2 \cos^2 \varphi} \\ \text{var}(\hat{\varphi}) &\geq \frac{\sigma^2}{2\mathcal{E}} \frac{1 - s \sin^2 \varphi - \rho^2 \cos^2 \varphi}{s(1 - s \sin^2 \varphi) - \mu^2 \sin^2 \varphi - s\rho^2 \cos^2 \varphi} \\ \text{MSAE} &= \frac{\sigma^2}{2\mathcal{E}} \frac{1 - \rho^2 \cos^2 \varphi}{s(1 - s \sin^2 \varphi) - \mu^2 \sin^2 \varphi - s\rho^2 \cos^2 \varphi} \end{aligned}$$

By Cauchy-Schwarz inequality,  $-1/2 \leq \mu \leq 1/2$ .  $\mu = \pm 1/2$  if and only if linear polarization is used ( $\mathbf{s}_{r1} = \text{real constant} \cdot \mathbf{s}_{r2}$ ).

#### B. Special Case: UWB Antenna with 2-dipoles, 1-loop.

Consider a three element receiver with two orthogonally located ultrawideband dipoles and a ultrawideband loop with colocated with the dipoles in the same plane. In this case, we have

$$B(\theta, \varphi) = \begin{bmatrix} -\sin \theta & \cos \theta \cos \varphi \\ \cos \theta & \sin \theta \cos \varphi \\ -\sin \varphi & 0 \end{bmatrix}$$

We call this the (2,1) antenna henceforth. We can get expressions in a similar way for this antenna structure. We omit the exact bound expressions for lack of space.

## V. OPTIMAL SIGNALS

We use the exact expressions for the variance lower bounds as a signal design criterion. The signal pair  $(\mathbf{s}_1, \mathbf{s}_2)$ , that minimizes the MSRE lower bound and makes it DOA independent are *optimal* for range estimation. Signals that minimize the MSAE lower bound and make it DOA independent are optimal for DOA estimation. We make the following observations

- For the tripole antenna, signals with  $\rho = 0$  (orthogonal) are optimal in the sense just described for range estimation. For the (2,1) antenna, signals with  $p = 1$  and  $\rho = 0$  are optimal for range estimation.
- For the tripole antenna, signals with  $\rho = \pm 1$ ,  $s = 1/2$ , and  $\mu = 0$  are optimal for DOA estimation. For the (2,1) antenna, signals with  $p = 1$ ,  $\rho = \pm 1$ ,  $s = 1/2$ , and  $\mu = 0$  are optimal for DOA estimation.

Linearized confidence region is defined as the volume of confidence ellipsoid of Wald's test (not developed in this paper, but will be presented elsewhere). The confidence region indicates the uncertainty volume for the location estimate when the parameters are  $(r, \theta, \varphi)$ , and can be written explicitly in terms of the CRB. This can be used as a criterion for optimal signal design by choosing signals that minimize that volume. We find that signals optimal in this sense are optimal in the sense of DOA estimation. So, we choose this as the design criterion for joint estimation of range and DOA.

The MSRE and MSAE lower bounds under this choice of signals are identical for both tripole and (2,1) antennas. (i.e., the Maximum Likelihood Estimator asymptotically achieves these bounds and gives the same performance in target localization for both the antennas). The lower bounds are given as:  $\text{MSAE} \geq 2/\text{SNR}$  and  $\text{MSRE} \geq c^2/(8\omega^2 \text{SNR})$ , where  $\text{SNR} = \mathcal{E}/\sigma^2$ . Choosing the signal pair such that  $\mathbf{s}_1(t) = A \cos \omega_s t$  for  $t \in [-\pi/\omega_s, \pi/\omega_s]$  and zero otherwise, and  $\mathbf{s}_2(t) = A \sin \omega_s t$  for  $t \in [-\pi/\omega_s, \pi/\omega_s]$  and zero otherwise, satisfies the optimization criterion. Since, these pulses are complex envelopes and modulate the carrier waveform  $e^{j\omega_c t}$  by choosing  $\omega_c/\omega_s = n + 1/2$ , where  $n$  is positive integer, we can ensure that modulated waveform is zero at the boundary. These waveforms satisfy the requirements for DOA independent angle estimation.

## VI. CONCLUSIONS

To demonstrate the advantages of using a polarimetric vector antenna instead of a single ultrawideband dipole or loop, we considered the beamforming problem as applied to EM source localization with receivers that use vector antennas. We derived an asymptotic expression for frequency domain CRB for a vector Gaussian process. This result generalizes the expression obtained in [16] for a scalar Gaussian random process with separable covariance structure to the case of vector signal observations from a proper stationary Gaussian random process. Exact expressions for the asymptotic CRB for range and direction of arrival estimation were derived. Signals that make the CRB's independent of the DOA were obtained for both range and DOA estimation. With either the MSRE or

MSAE or the volume of confidence criterion, signals that are optimal for the 2,1 antenna are also optimal for the tripole. Further, the performances for both the antennas are the same under the optimal signal choice.

#### APPENDIX

In this appendix, we present results on the asymptotic behavior of block Toeplitz matrices which are used in Sec. II. Consider a sequence of block Toeplitz matrices

$$R_n = \begin{bmatrix} T_0 & T_{-1} & \cdots & T_{-(n-1)} \\ T_1 & T_0 & \cdots & T_{-(n-2)} \\ \vdots & \vdots & \ddots & \vdots \\ T_{n-1} & T_{n-2} & \cdots & T_0 \end{bmatrix}$$

where  $\{T_k\}$  is a sequence of  $r \times s$  complex matrices. Denote the  $ij$ -th element of  $T_k$  by  $t_k^{ij}$ .

**Lemma A1:** If  $\{T_k\}$  is such that  $\sum_{k=-\infty}^{\infty} |t_k^{ij}| < \infty$  for all  $i$  and  $j$ , then  $R_n$  is asymptotically equivalent to the block circulant matrix

$$C_n = (W_n \otimes I_r)^H D_n(T) (W_n \otimes I_s),$$

where  $W_n$  is the DFT matrix,  $D_n(T)$  is the block diagonal matrix, and  $T(\omega)$  is the discrete Fourier Transform of the matrix sequence  $\{T_k\}$

$$T(\omega) = \sum_{k=-\infty}^{\infty} T_k e^{-jk\omega}.$$

*Remarks:* For  $r = s = 1$ , the result was proved by Gray [18]. For the particular case  $r = s > 1$ , an alternative asymptotic expression is stated without proof by Gazzah *et al* [2]. It can be shown that the expression in [2] is equivalent to (6); however, we shall omit this and instead give a direct proof of (6) since it is simpler, a bit more general, and makes the paper more self-contained.

*Proof:* Let  ${}_k I_{n,r}$  denote an  $n \times rn$  matrix such that  $[{}_k I_{n,r}]_{ij} = \delta_{j,k+ir}$ . It is straightforward to prove that the following properties hold for any  $rn \times sn$  matrix  $A$ :

- (A1)  ${}_k I_{n,r} A$  is the submatrix of  $A$  comprising the  $n$  rows  $k, k+r, \dots, k+(n-1)r$ .
- (A2)  ${}_k I_{n,r}^T {}_k I_{n,r} A$  is equal to  $A$  with all rows zeroed except  $k, k+r, \dots, k+(n-1)r$ .
- (A3)  $A = \sum_{i=1}^r \sum_{j=1}^s i I_{n,r}^T A j I_{n,s}^T$
- (A4)  $B \otimes I_r = \sum_i i I_{n,r}^T B i I_{n,r}$  for any  $n \times n$  matrix  $B$

To prove (6), observe that  ${}_i I_{n,r} R_n j I_{n,s}^T$  is an  $n \times n$  Toeplitz matrix formed from the scalar sequence  $t_k^{ij}, k = 0, \pm 1, \dots$  for all  $i$  and  $j$ . From [18], we therefore have  ${}_i I_{n,r} R_n j I_{n,s}^T \sim W_n^H D_n(t^{ij}) W_n$ . Observing that  $D_n(t^{ij}) = {}_i I_{n,r} D_n(T) j I_{n,s}^T$ ,

we conclude that

$$\begin{aligned} R_n &\stackrel{(A3)}{=} \sum_{ij} {}_i I_{n,r}^T {}_i I_{n,r} R_n j I_{n,s}^T {}_j I_{n,s} \\ &\sim \sum_{ij} {}_i I_{n,r}^T W_n^H D_n(t^{ij}) W_n j I_{n,s} \\ &= \sum_{ij} {}_i I_{n,r}^T W_n^H {}_i I_{n,r} D_n(T) j I_{n,s}^T W_n j I_{n,s} \\ &= \left( \sum_i {}_i I_{n,r}^T W_n^H {}_i I_{n,r} \right)^H D_n(T) \left( \sum_j j I_{n,s}^T W_n j I_{n,s} \right) \\ &\stackrel{(A4)}{=} (W_n \otimes I_r)^H D_n(T) (W_n \otimes I_s), \end{aligned}$$

where the second step follows by observing  $A_n \sim C_n$  and  $B_n \sim D_n$  implies  $A_n + B_n \sim C_n + D_n$ .

#### REFERENCES

- [1] Federal Communications Commission, "FCC affirms rules to authorize the deployment of ultra-wideband technology," FCC press release, Feb. 13, 2003 (online at <http://hraunfoss.fcc.gov>)
- [2] H. Gazzah, P. A. Regalia and J-P. Delmas, "Asymptotic eigenvalue distribution of block-Toeplitz matrices and application to blind SIMO channel identification," *IEEE Trans. Inform. Theory*, vol. 47, no. 3, pp. 1243–1250, March 2001.
- [3] E. Ertin and L. Potter, "Polarimetric imaging wide band synthetic aperture radar," *IEE Proceedings – Radar, Sonar, and Navigation*, vol. 145, no. 5, pp. 275–280, Oct. 1998.
- [4] S. M. Kay, *Fundamentals of Statistical Signal Processing: Estimation Theory*, Englewood Cliffs, NJ: Prentice-Hall, 1993.
- [5] C.-C. Chen, M. Higgins, K. O'Neill and R. Detsch, "UWB fully-polarimetric GPR classification of sub-surface unexploded ordnance", *IEEE Transaction on Geoscience and Remote Sensing*, vol. 39, no. 6, pp. 1221–1230, June 2001.
- [6] L. Carin, R. Kapoor and C. Baum, "Polarimetric SAR imaging of buried landmines," *IEEE Trans. Geosci. Remote Sensing*, vol. 36, pp. 1985–1988, Nov. 1998.
- [7] A. Nehorai and E. Paldi, "Vector-sensor array processing for electromagnetic source localization," *IEEE Tran. Signal Proc.*, vol. 42, no. 2, pp. 376–398, Feb 1994.
- [8] Y. Huang, A. Nehorai, and G. Friedman, "Mutual coupling of two collocated orthogonally oriented circular thin-wire loops," to appear in *IEEE Trans. Antennas and Propagation*, vol. AP-51, Apr. 2003.
- [9] C.-C. Ko, J. Zhang, and A. Nehorai, "Separation and tracking of multiple broadband sources with one electromagnetic vector sensor," *IEEE Trans. on Aerospace and Electronic Systems*, vol. 38, pp. 1109–1116, July 2002.
- [10] H. F. Harmuth, *Origins and Use of Nonsinusoidal Waves in Radar and Radio Communication*, New York: Academic Press, 1981.
- [11] G. Hatke, "Performance analysis of the superCART antenna array," MIT Lincoln Lab, Lexington, MA, Project Rep. AST-22, March 1992.
- [12] M. G. M. Hussain and M. J. Yedlin, "Active-array beamforming for ultra-wideband impulse radar," in *Proc. IEEE 2000 Int. Radar Conf.*, Alexandria, VA, pp. 267–272, May 2000.
- [13] F. D. Neeser and J. L. Massey, "Proper complex random processes with applications to information theory," *IEEE Trans. Inform. Theory*, vol. 39, no. 4, pp. 1293–1302, July 1993.
- [14] M. Kanda, "An electromagnetic near-field sensor for simultaneous electric and magnetic field measurements," *IEEE Trans. Electromagn. Compat.*, vol. EMC-26, pp. 102–110, Aug. 1984.
- [15] J. D. Taylor, *Introduction to Ultra-wideband Radar Systems*, Boca Raton, Florida: CRC Press, 1995.
- [16] A. Zeira, and A. Nehorai, "Frequency Domain Cramer-Rao bound for Gaussian Processes", *IEEE Tran. on Acoustics, Speech and Signal Processing*, Vol. 38, No. 6, June 1990.
- [17] G. A. Deschamps, "Geometrical representation of the polarization of a plane electromagnetic wave," *Proc. IRE*, vol. 39, pp. 540–544, May 1951.
- [18] R. M. Gray, "On the asymptotic eigenvalue distribution of Toeplitz matrices," *IEEE Trans. Inform. Theory*, vol. IT-18, no. 3, pp. 867–881, May 1978.